ON THE EQUIVALENCE OF MEASURED AND AVERAGED PRESSURES IN POROUS MEDIA

BERENTSEN, C.W.J., S.M. HASSANIZADEH[1]

[1]*Utrecht University, Department of Earth Sciences, Environmental Hydrogeology group, Budapestlaan 4, 2508 TA, Utrecht, The Netherlands*

ABSTRACT

In a numerical study we investigated the relation between the pressure measured by an in-situ pressure transducer and some area-average of the pressure distribution over that part of the porous media that is in contact with the transducer. We considered the intrinsic phase average, the arithmetic and intrinsic arithmetic average and the centroid phase pressure. It appears that the transducer generates a tiny by-pass flow that for two-phase flow may significantly effect the saturation distribution over the contact area. This disturbance is larger for larger membrane permeability and for larger pressure gradients over the transducer height. It causes the intrinsic phase average pressure to give less accurate predictions under stationary flow conditions, as it overestimates the impact of the phase volume on the pressure response. However, for all practical situations and sufficiently small membrane permeabilities our model suggests that the pressure error by the averages will remain within a few percents for stationary two-phase flow in homogeneous media. In contrast all averages show errors larger than 10% in a drainage experiment at a 10kPa pressure drop over the transducer height.

1. INTRODUCTION

Fluid pressure in porous media is commonly measured by means of a manometer or a pressure transducer. The measurement is actually done on a body of fluid just outside the porous medium, which is in hydraulic contact with the fluid just inside the porous medium. It is almost always assumed that the measured fluid pressure is equal to some volumetric or area-averaged phase pressure of the fluid inside the porous medium. As far as we know this major assumption however, has never been verified. In this work we will discuss this issue and address its potential significance to the study of two-phase flow.

In this work, we first consider single-phase flow in a "perfectly" homogeneous porous medium under variable flow conditions. Subsequently, we analyse the behaviour when the medium has a constant porosity gradient. These results can be compared to a recently developed theory on centroid-averaged pressures by Nordbotten et al (2006). Next, we consider two-phase flow in a column where the two fluid pressures are measured using selective pore pressure transducers. We first discuss the results for quasi-static two-phase flow and end this work with the analysis of a dynamic drainage experiment. We have found out that the pressure "sensed" by the pressure transducer is significantly different from various forms of average pressure, when there is a gradient in porosity and/or saturation.

2. LOCAL TWO-PHASE FLOW MODEL

At the macroscopic or REV scale, the governing equations for two-phase incompressible flow are the mass balance for each phase α (with α=(w) for water or (n) for DNAPL) (Helmig, 1997):

$$\frac{\partial S^{\alpha}}{\partial t} + \frac{1}{\phi}\nabla \bullet \mathbf{u}_{\alpha} = 0 \tag{1}$$

and Darcy's law stating the relation between the Darcy phase velocity ($\mathbf{u}_{\alpha}$) and the driving phase potential Φ^{α}, defined by $\nabla\Phi^{\alpha} = \nabla p^{\alpha} - \rho^{\alpha} g \mathbf{e}_z$:

$$\mathbf{u}_{\alpha} = -\Lambda_{\alpha}\nabla\Phi^{\alpha}, \qquad \Lambda_{\alpha} = K k_r^{\alpha} / \mu^{\alpha} \tag{2}$$

Here, S is the saturation, K is the intrinsic permeability tensor, Λ is the total phase mobility, k_r is the relative permeability, μ is the viscosity, ρ is the density, ϕ is the porosity, g is the gravitational acceleration and z is the elevation. By definition both phase saturations add up to 1. In addition to (1) and (2), we need an equation that relates the pressures of the two phases. We assume that the local capillary pressure is defined as a (static) equilibrium function relation between the DNAPL and water pressure (Bear, 1972):

$$p^n - p^w = p^c_{stat}\left(S^n\right) \tag{3}$$

in which the static capillary pressure function p^c_{stat} is assumed to be a unique function of the saturation. We assume that Brooks-Corey formula prescribes the capillary pressure relation:

$$p_c(S^e) = p_d (S^e)^{-1/\lambda} \tag{4}$$

Here, p_d is the entry pressure, λ is the sorting factor and $S^e = (S^w - S^w_{res})/(1 - S^w_{res} - S^n_{res})$ is the effective wetting phase saturation with S^w_{res} being the residual wetting phase saturation and S^n_{res} the residual non-wetting phase saturation. Relative permeabilities for the wetting phase and non-wetting phase are assumed to be directly related to the static capillary pressure function:

$$\begin{aligned} k_r^w &= (S^e)^{(2+3\lambda)/\lambda} \\ k_r^n &= \left(1-(S^e)^2\right)\left(1-(S^e)^{(2+\lambda)/\lambda}\right) \end{aligned} \tag{5}$$

Single phase fluid flow is simulated by this two-phase model by simply adjusting the boundary and initial conditions.

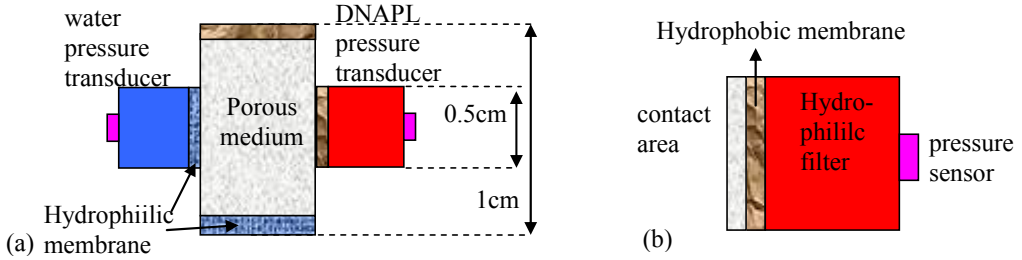

FIGURE 1: (a) Virtual set-up and (b) close up of the DNAPL transducer

3. VIRTUAL EXPERIMENTAL SET-UP

We consider two-phase flow in a soil column, where a homogeneous soil sample is placed between a hydrophobic membrane (top) and hydrophilic membrane (bottom), Fig 1a. This set-up is similar to the one used in column experiments described by Hassanizadeh et al. (2004) In drainage experiments, the soil is initially filled with water and the DNAPL pressure at the top of the set-up is increased to cause infiltration into the soil. Although this set-up simulates one-dimensional flow across the soil sample, we will have a two-dimensional situation because of the presence of the pressure transducers. The sample is connected at the left to a water-wet pressure transducer and at the right to a DNAPL-wet pressure transducer. A selective α-phase pore pressure transducer consists of a low-permeable membrane that is in contact with the soil, a highly permeable filter that serves one side as support for the membrane and on the other side is in contact with the real pressure sensor (Fig 1b). A detailed description of the selective pore pressure transducer is given by Oung and Bezuijen (2002 and 2004). The filter and the membrane are α-phase wet and saturated with the α-phase. Ideally no fluid should cross a membrane while pressure is still "transferred" over the membrane. In reality, however, each membrane will have a small non-zero permeability allowing for a tiny fluid flow.

3.1 Measured pressure & average pressure

The permeability of each filter is taken sufficiently large such that potential gradients in the filter are negligible compared to potential gradients in the remainder of the set-up. The sensor pressure refers to the pressure exerted by the fluid in the filter on the sensor. We assume that the pressure in each α-phase transducer is only related to the contact area of the α-phase membrane with the α-phase in the porous sample. Moreover, we do not consider film flow and for primary drainage we assume that there is no by-pass flow from the transducer to the sand downstream of the fluid front. We investigate whether the sensor pressure can be related to some volume average of the pressures over a thin strip alongside the membrane (see Fig 1b). We consider the arithmetic average $\langle\ \rangle_A$, intrinsic arithmetic average $\langle\ \rangle_{A^\alpha}$ and intrinsic phase volume average $\langle\ \rangle_{S^\alpha}$ defined as (see also Manthey et. al 2005):

$$\left\langle p^\alpha \right\rangle_A = \frac{\int_V p^\alpha dV}{\int_V dV}, \qquad \left\langle p^\alpha \right\rangle_{A^\alpha} = \frac{\int_{V^\alpha} p^\alpha dV}{\int_{V^\alpha} dV}, \qquad \left\langle p^\alpha \right\rangle_{\phi S^\alpha} = \frac{\int_V \phi S^\alpha p^\alpha dV}{\int_V \phi S^\alpha dV} \tag{6}$$

In addition we consider the centroid phase pressure that is recently proposed by Norbotten et al. (2006) and defined as:

$$\left\langle p^\alpha \right\rangle_C = \left\langle p^\alpha \right\rangle_{\phi S^\alpha} - (\langle \mathbf{x} \rangle_{\phi S^\alpha} - \langle \mathbf{x} \rangle_A)^T \bullet \left(\nabla \langle \mathbf{x} \rangle_{\phi S^\alpha} \right)^{-1} \bullet \nabla \left\langle p^\alpha \right\rangle_{\phi S^\alpha} \tag{7}$$

Where needed we compare the results to the in-situ averaged saturation. This is the volume averaged of the saturation over the volume between the transducers.

$$S^\alpha_{in,situ} = \frac{\int_{V_{sand\_between\_transducers}} \phi S^\alpha dV}{\int_{V_{sand\_between\_transducers}} \phi dV} \tag{8}$$

4. NUMERICAL MODEL

In our two-dimensional (2D) numerical model, we solve the following set of equations for the non-wetting phase saturation S^n and the two phase potentials Φ^n and Φ^w, simultaneously:

$$\begin{aligned} +\phi\partial_t S^n - \nabla(\Lambda^n \nabla\Phi^n) &= 0 \\ -\phi\partial_t S^n - \nabla(\Lambda^w \nabla\Phi^w) &= 0 \\ \Phi^n - \Phi^w - [\rho^n - \rho^w]gz &= p^c_{stat} \end{aligned} \tag{9}$$

We solve (9) iteratively using the implicit Newton-Raphson method. In the z direction harmonic average absolute permeabilities and upwind weighted phase relative permeabilities are used at the interfaces, in the x-direction harmonic averaged total phase mobilities. Contrary to upwind weighting, harmonic averages preserve symmetry of flow into the transducers in quasi static two-phase flow. The time step used is variable and is constrained by a maximum allowable saturation change of 0.1 per gridblock per timestep.

5. TRANSDUCER ANALYSIS FOR SINGLE-PHASE FLOW

5.1 Initial and boundary conditions

For single phase flow we assume that the soil sample as well as the top and bottom membranes are all hydrophilic and fully water saturated. We specify Dirichlet boundaries at the top and bottom as follows:

$$p^w_{bottom} = 0, \qquad p^w_{top} = \Delta p \tag{10}$$

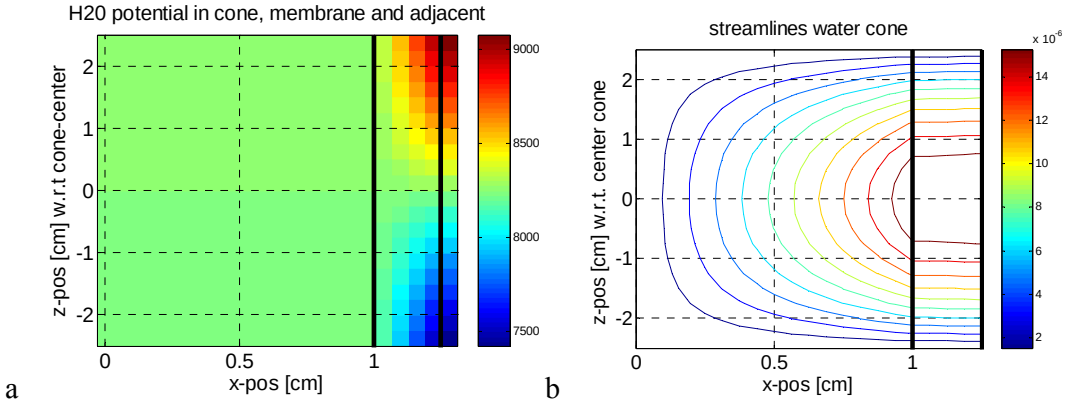

a b

FIGURE 2: (a) Potential distribution and (b) streamline pattern in water transducer and in porous medium adjacent to the hydrophilic membrane for single phase flow.

5.2 Homogeneous sand

For homogeneous sand, all pressure averages defined in (section 3.1) give the same value. Fig 2a shows that the (nearly) constant water potential in the cone is the same as the water potential in the middle of the sand strip. Fig 2b shows that the streamlines of the Darcy flux are nicely symmetrical around the z-centre of the cone.

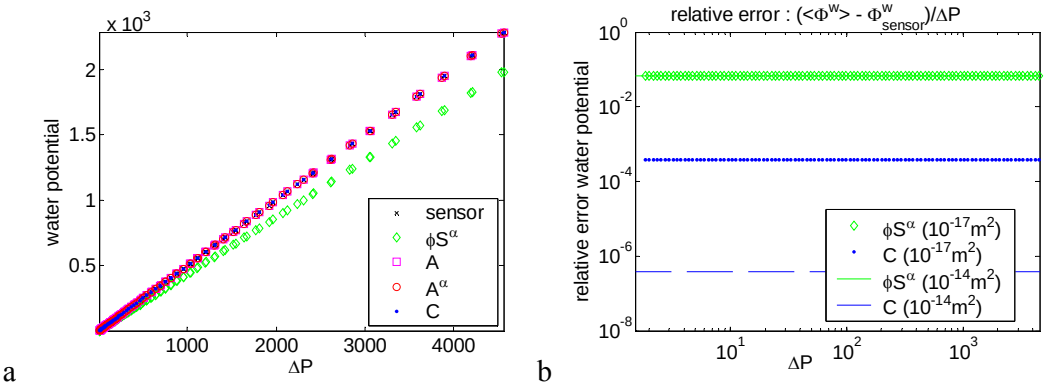

FIGURE 3: (a) comparison between average water potential and sensor potential (b) relative error of intrinsic phase average and centroid potential for $K_{membrane}=10^{-14}m^2$ and $10^{-17}m^2$

5.3 Sand with constant porosity gradient

For sand with a constant porosity gradient ($\Delta\phi=0.8$ over 1cm), the potential distribution and the Darcy flow streamline pattern are the same for homogeneous sand (Fig 2). Fig 3a shows that all potential averages seem to indicate the same potential as the sensor, except for the intrinsic phase average potential. Fig 3b shows the deviation of the intrinsic phase averaged and centroid phase potential from the sensor potential for membrane permeability $K=10^{-14}$ m^2 and $K=10^{-17}m^2$. The intrinsic phase averaged over estimates the impact of the phase volume on the pressure behavior and gives a constant error of 6.7%. The deviation in the (1D) centroid phase pressure results from the by-pass flow through the transducer (significant 2nd order derivatives) and vanishes in the limit of the membrane permeability to zero. The error within the arithmetic averages is in the order of the machine precision for this case.

6. TRANSDUCER ANALYSIS FOR TWO-PHASE FLOW

6.1 Concurrent two-phase flow through homogenous sand

6.1.1 Initial and boundary conditions

We simulate concurrent flow of wetting and non-wetting phases. For this experiment the top and bottom membrane are assumed to have the same properties as the soil sample. Each phase has a constant global pressure drop (ΔP) over the entire sample height. Moreover, the phase pressures difference is the same (p^c_{global}) at both boundaries:

$$\begin{aligned} p^w_{top} &= \Delta p & p^w_{bottom} &= 0 \\ p^n_{top} &= p^w_{top} + p^c_{global} & p^n_{bottom} &= p^w_{bottom} + p^c_{global} \end{aligned} \qquad (11)$$

The initial sand saturation is derived by inverting the capillary-pressure saturation difference for $p^c = p^c_{global}$. In the example we use $\Delta p = 25$kPa and $p^c_{global} = 1.2\,p^d_{sand}$.

6.1.2 Comparison of averaged pressures with sensor pressure

For small membrane permeability ($K_{membrane}=5\text{x}10^{-15}m^2$ $K_{sand}=3\text{x}10^{-12}m^2$) we obtain streamline and pressure profiles that look similar to the profiles for single phase flow (Fig 2).

However, each transducer generates a small by-pass flow that disturbs the symmetry (Fig 4). The disturbance resulting from the by-pass flow is larger for larger global pressure drop as shown by Fig 4a. The disturbance is also larger for larger membrane permeability (Fig 4b). Part of the water is abstracted from the main fluid flow along the transducer and flows through the transducer. This causes the water saturation to decrease in the sand adjacent to the upstream side of the transducer. Similarly the water leaving the transducer causes the downstream saturation to be larger. In our case this effect is stronger at the water transducer due to the larger mobility of the DNAPL phase.

Fig 5a and b show that the difference in water- and capillary pressure ($< p^n > - < p^w >$) between the averages and the sensor increases as function of the global potential drop over entry pressure ratio ($\Delta P/p^d$). Both figures show that the intrinsic phase average pressure gives errors that are 1 to 2 orders of magnitude larger than the other averages. However, for the water pressure even the intrinsic phase averaged remains smaller than 2% (Fig 5a). Fig 5b shows that a small error in the phase pressures may still produce a large(r) error in the capillary pressure when the pressure gradient over the height of the transducer is large. At ratio ($\Delta P/p^d$ =5) the relative error in the capillary pressure by the intrinsic phase averaging reaches upto to 10%, while the relative error by the other averages remains sufficiently small. For ratios ($\Delta P/p^d$) smaller than one all errors remains within a 1% limit.

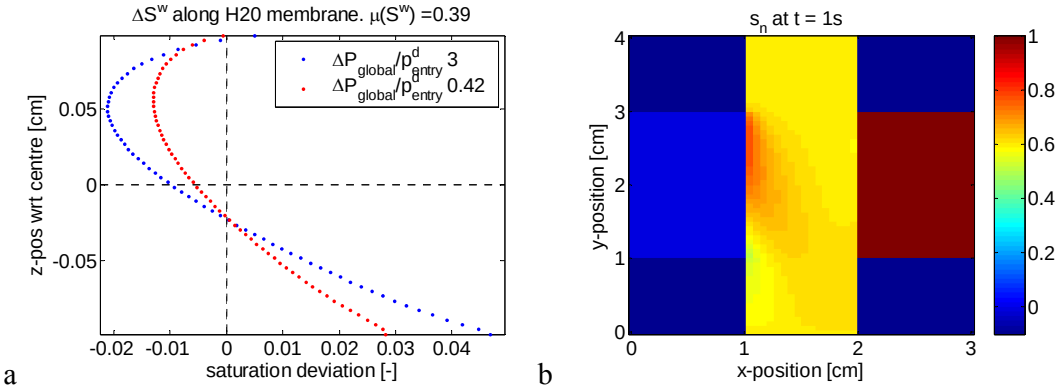

FIGURE 4: Disturbance of saturation distribution by the transducer. (a) deviation of saturation from mean saturation in grid blocks alongside the water transducer for $K_{membrane}$=5x10^{-15}m^2 (b) DNAPL saturation in set-up for K=5x10^{-14} m^2 and ΔP=20 kPa

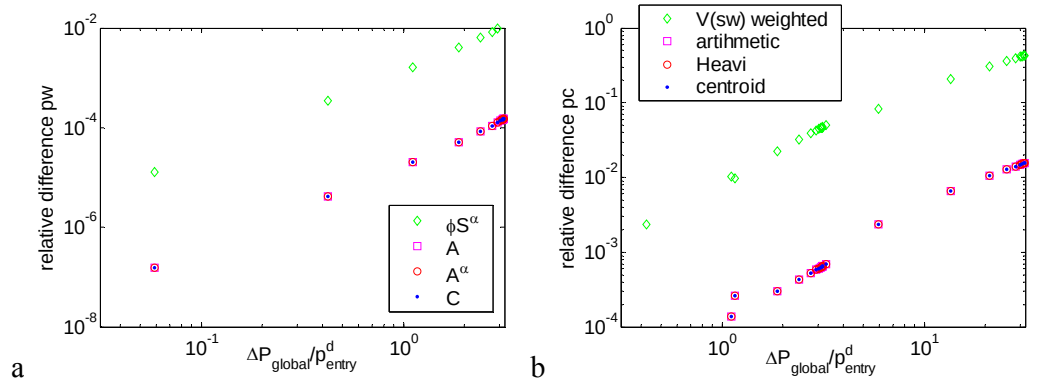

FIGURE 5: Pressure difference between averaged pressures and sensor pressures as function of the ratio $\Delta P/p^d$. Left capillary pressure right water pressure (for K=5x10^{-15}).

6.2 Two-phase drainage at constant porosity and permeability

6.2.1 Initial and boundary condition

Initially the soil sample and hydrophilic bottom membrane are fully water saturated. The hydrophobic top membrane is fully oil saturated. At the top boundary, a no-flux boundary is imposed for the water phase and a Dirichlet condition for the DNAPL. At the bottom, a no-flux boundary is imposed for the DNAPL phase and a time varying Dirichlet condition for the water phase that increases proportional to the water flux leaving the set-up:

$$\begin{aligned} q^w_{top} &= 0 & \frac{\partial p^w_{bottom}}{\partial t} &= k\,|\,u^w_{bottom}\,|\,, \quad p^w_{bottom}(0) = 0 \\ p^n_{top} &= \Delta P & q^n_{bottom} &= 0 \end{aligned} \tag{12}$$

6.2.2 Comparison of sensor and averaged pressures

In this case we consider a membrane permeability $K_{membrane}=10^{-16}\text{m}^2$ and pressure drop $\Delta P=20\text{kPa}$. Fig 6 gives an example of the resulting asymmetric streamline patterns of the flow through the DNAPL transducer. Fig 7a and b show the DNAPL and capillary pressure as function of the (in situ) saturation computed by the sensors and by the various pressure averages. Fig 8 shows the difference in the capillary pressure resulting from the averages relative to the capillary pressure by the sensor as function of time. For the considered flow conditions, the deviation of the averaged pressure from the sensor pressure is large, as long as the fluid front is passing the transducer. The arithmetic average and centroid phase pressure even produce unacceptably large errors (>100%), while the intrinsic phase volume average and intrinsic phase arithmetic stay within a 10% margin. When the fluid front has passed the transducer the deviation by the centroid and arithmetic averages rapidly drop to insignificance. In contrast, the intrinsic phase volume average remains temporarily at a deviation of several percents.

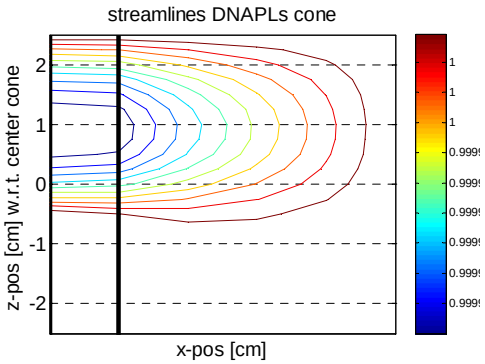

FIGURE 6: Streamline pattern in the DNAPL transducer for fluid front halfway transducer

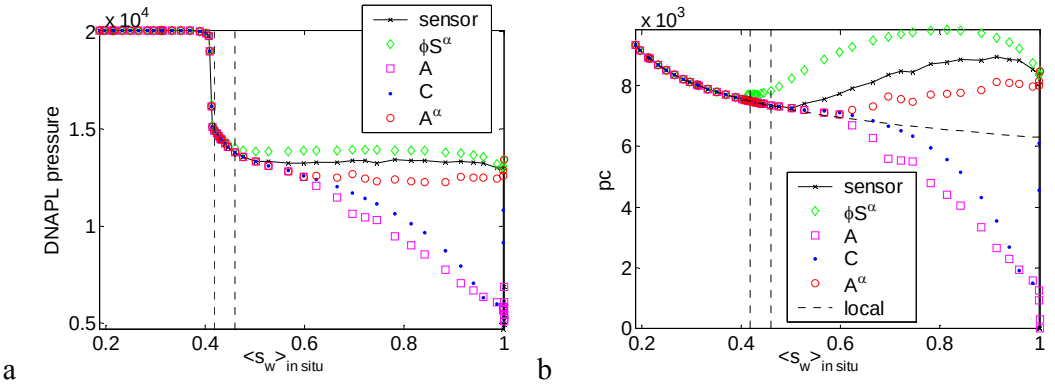

FIGURE 7: (a) DNAPL and (b) capillary pressure as function of in-situ averaged saturation. For decreasing saturation, the vertical dashed lines indicate the moment the fluid front reaches the lower end of the transducer and the bottom.

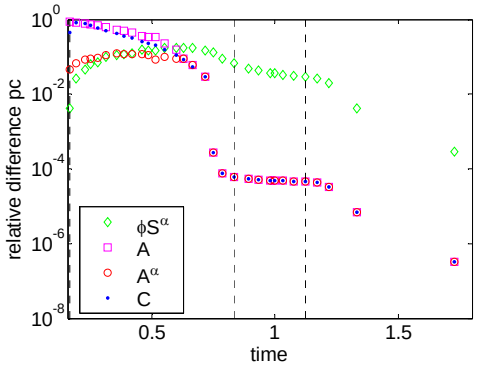

FIGURE 8: Relative difference in capillary pressure between the average pressures and the sensor pressure as function of time.

7. DISCUSSION

The question: "what does a transducer measure" is closely related to the question "what is averaged pressure" and is far from answered yet. It may be even more complicated as the presence of the transducer disturbs the flow it is attempting to measure. So far, we did not consider the effect of the size of the transducer (averaging window), the impact of heterogeneity and the impact of the assumptions. We only investigated to a small extent the impact of the membrane permeability and the pressure gradient along the transducer.

8. CONCLUSIONS

In a numerical study on soil with constant permeability we investigated the relation between the pressure "measured" by a selective in-situ pressure transducer and the averaged pressure over a small strip adjacent to the transducer. Our preliminary conclusions are:

Under "stationary" two-phase flow conditions the presence of the transducer disturbs the flow and changes the saturation distribution along the transducer. This disturbance is larger

for larger membrane permeability and larger pressure gradients over the height of the transducer.

- For single phase flow in a soil with constant porosity gradient, the arithmetic averages give the same pressure as the sensor. The deviation by the centroid phase pressure is very small and vanishes for zero membrane permeability. At an extreme porosity gradient $\Delta\phi$=0.8/cm, the intrinsic phase average gives a systematic error of 6.7%.

- In most realistic scenarios, all considered averages will sufficiently accurately reproduce the pressure behaviour for stationary two-phase flow conditions in homogeneous soil, provided that the membrane permeability is sufficiently small.

- Due to the disturbance of the saturation profile along the transducer the intrinsic phase volume average gives the least accurate prediction under stationary conditions, as it overestimates the impact of the phase volume on the pressure behaviour.

- In the considered two-phase drainage experiments none of the considered pressure averages accurately reproduce the sensor pressures as long as the fluid front passes the transducer.

Acknowledgements

We would like to thank Jan Nordbotten and Helge Dahle of Bergen University and Mike Celia of Princeton University for fruitful discussions. Moreover, we thank Rainer Helmig of Stuttgart University for valuable help with the numerical scheme.

This research has been partially supported by the Netherlands Organisation for Scientific Research (NWO). Also, the support from the Utrecht Centre of Geosciences (UCG) has been greatly appreciated.

References

- Bear, J., Dynamics of Fluids in Porous Media, Dover Publications, New York, 1972.
- Hassanizadeh, S.M., M.A. Celia, and H.K. Dahle, "Dynamic effects in the capillary pressure-saturation relationship and their impacts on unsaturated flow," Vadose Zone Journal, 1, pp. 38-57, 2002.
- Hassanizadeh, S.M., Oung, O., and S. Manthey, Laboratory experiments and simulations on the significance of non-equilibrium effect in the capillary pressure-saturation relationship, in: Unsaturated Soils: Experimental Studies. Proceedings of the International Conference: From Experimental Evidence towards Numerical Modeling of Unsaturated Soils, Weimar, Germany, September 18-19, 2003, Volume 1, Ed. T. Schanz, Springer Verlag, Berlin, pp. 3-14, 2004.
- Helmig, R., Multiphase Flow and Transport Processes in the Subsurface, Springer, Berlin, 1997.
- Manthey, S., S.M. Hassanizadeh, and R. Helmig, "Macro-scale dynamic effects in homogeneous and heterogeneous porous media," Transport in Porous Media, 58, no.1-2, pp. 121-145, 2005.
- Nordbotten J. M., M. A. Celia, H. K. Dahle, S. M. Hassanizadeh, Interpretation of Pressure in Darcy's Law, submitted to Water Resources Research, 2006.
- Oung, O. and A. Bezuijen, "Development of selective pore pressure transducers and their use to check the validity of 'classical' capillary pressure saturation curves", Proceedings of Int. Conf. on Physical Modelling and Geotechnics ICPMG'02, Phillips, Guo & Popescu (eds.), Swets & Zeitlinger Lisse, ISBN 90 5809 389 1, St Johns (Canada), pp 95-100, 2002.
- Oung, O. & Bezuijen, A. (2003) 'Calibration and validation of developed selective pore pressure transducers for used in model tests', Int. J. of Physical Modelling in Geotechnics, 2004.